

Contents lists available at [SciVerse ScienceDirect](http://SciVerse.ScienceDirect.com)

Biochimica et Biophysica Acta

journal homepage: www.elsevier.com/locate/bbamem

Membrane and lipopolysaccharide interactions of C-terminal peptides from S1 peptidases

Shalini Singh ^a, Gopinath Kasetty ^b, Artur Schmidtchen ^b, Martin Malmsten ^{a,*}^a Department of Pharmacy, Uppsala University, SE-75123, Uppsala, Sweden^b Division of Dermatology and Venereology, Department of Clinical Sciences, Lund University, SE-221 84 Lund, Sweden

ARTICLE INFO

Article history:

Received 8 February 2012

Received in revised form 23 March 2012

Accepted 26 March 2012

Available online 2 April 2012

Keywords:

Antimicrobial peptide

Dual polarization interferometry

Ellipsometry

Lipopolysaccharide

Liposome

Membrane

ABSTRACT

The mechanisms underlying antimicrobial and anti-endotoxic effects were investigated for a series of structurally related peptides derived from the C-terminal region of S1 peptidases. For this purpose, results on bacterial killing were compared to those on peptide-induced liposome leakage, and to ellipsometry and dual polarization interferometry results on peptide binding to, and disordering of, supported lipid bilayers. Furthermore, the ability of these peptides to block endotoxic effects caused by bacterial lipopolysaccharide (LPS), monitored through NO production in macrophages, was compared to the binding of these peptides to LPS, and to secondary structure formation in the peptide/LPS complex. Bacteria killing, occurring through peptide-induced membrane lysis, was found to correlate with liposome rupture, and with the extent of peptide binding to the lipid membrane, no adsorption threshold for peptide insertion being observed. Membrane and LPS binding was found to depend on peptide net charge, illustrated by LPS binding increasing with increasing peptide charge, and peptides with net negative charge being unable to lyse membranes, kill bacteria, and block LPS-induced endotoxic effect. These effects were, however, also influenced by peptide hydrophobicity. LPS binding was furthermore demonstrated to be necessary, but not sufficient, for anti-endotoxic effect of these peptides. Circular dichroism spectroscopy showed that pronounced helix formation occurs in peptide/LPS complexes for all peptides displaying anti-endotoxic effect, hence potentially linked to this functionality. Similarly, ordered secondary structure formation was correlated to membrane binding, lysis, and antimicrobial activity of these peptides. Finally, preferential binding of these peptides to LPS over the lipid membrane was demonstrated.

© 2012 Elsevier B.V. All rights reserved.

1. Introduction

The innate immune system constitutes a first line of defense against invading microbes. Thus, antimicrobial peptides (AMPs) exert direct bactericidal effects, but may also display immunomodulatory functions, e.g., chemotaxis, angiogenesis, and anti-endotoxic effects [1–5]. Among several classes of such peptides, we have investigated anti-inflammatory as well as direct antimicrobial actions of peptides derived from coagulation-related proteins. For example, C-terminal peptides of human thrombin have been identified as a novel class of host defense peptides with antimicrobial as well as anti-inflammatory properties [6,7]. Such peptides not only display potent antimicrobial action through direct membrane disruption, but also binding to lipopolysaccharide (LPS) from Gram-negative bacteria, and are able to reduce LPS-induced inflammatory responses, evidenced from NO production in macrophages, as well as from results in animal models of septic shock induced by LPS [6] or bacteria [7].

In Gram-negative bacteria, LPS (also referred to as endotoxin) constitutes the major component of the outer leaflet of the outer bacterial membrane, where it covers >70% of the membrane [8] (Supporting material, Fig. S1a). Through this, AMPs and host defense peptides encounter an LPS barrier, which will have to be passed in order to reach the inner plasma membrane of the bacteria. LPS consists of a lipid component (lipid A), a core oligosaccharide region, and an outer (O-antigen) polysaccharide region [9] (Fig. S1b). Through phosphate and carboxyl moieties, LPS is negatively charged. Through the combined action of lipid A and the carbohydrate region, LPS is able to bind cationic and amphiphilic AMPs [10]. While structure–activity–relationship investigations have been extensively investigated with regard to AMP–membrane interactions and resulting antimicrobial function, studies on how peptide physicochemical properties such as length, charge (distribution), hydrophobicity (distribution), and secondary structure affect peptide–LPS interaction and resulting anti-endotoxic effects, are quite few in literature, as are studies on the interplay between, and relative importance of, AMP binding to LPS and lipid membranes [11–17]. In order to address this, we here report on investigations of membrane and LPS interactions for a series of peptides derived from the S1 peptidase family.

* Corresponding author. Tel.: +46 184714334; fax: +46 184714377.
E-mail address: martin.malmsten@farmaci.uu.se (M. Malmsten).

From a structural perspective, C-terminal peptides of thrombin, as well as those from related coagulation factors, are characterized by the pattern sequence X-[PFY]-X-[AFILV]-[AFY]-[AITV]-X-[ILV]-X(5)-W-[IL]-X(5,26) [18]. Strikingly, this evolutionary well-preserved sequence pattern can be found also in the functionally diverse family of S1 peptidases. Given this, as well as the direct antimicrobial and anti-inflammatory properties of C-terminal thrombin peptides, we previously demonstrated that a wide range of C-terminal S1-derived peptides share characteristics common with thrombin-derived C-terminal peptides, including direct antimicrobial effects due to membrane rupture and potent immunomodulatory effects [18].

While clear biological effects were thus demonstrated for both thrombin- and S1-derived C-terminal peptides, the underlying mode of action remains unclear. Although this most likely involves a series of biological functions in the complex and interconnected coagulation and inflammatory cascades, a natural starting point for such investigations is the peptide interaction with bacterial membranes and bacterial lipopolysaccharides. Given the cationic and amphiphilic nature of many antimicrobial and host defense peptides, it is not entirely unexpected that these may bind to bacterial and fungal lipopolysaccharides. Indeed, several studies have demonstrated such interactions qualitatively, and peptide scavenging by LPS has also been suggested as a mechanism by which such peptides counteract endotoxic responses triggered by LPS [11]. Despite this, quantitative aspects of the interaction between host defense peptides and LPS, and on how this may influence membrane interactions, and vice versa, remain relatively sparse in literature. Given this, as well as the previously demonstrated antimicrobial and anti-inflammatory properties of S1-derived C-terminal peptides [18], we here report on investigations of the interaction of a series of such peptides with lipid membranes and LPS, by combining studies on membrane rupture (liposome leakage), peptide binding to lipid membranes and LPS (ellipsometry and dual polarization interferometry; DPI), and peptide conformation on binding to liposomes and LPS (CD spectroscopy). Results from these model system investigations are furthermore compared to leakage induction in bacteria, bacteria killing, as well as anti-endotoxic effects of these peptides.

2. Experimental

2.1. Peptides

Peptides (Table 1) were synthesized by Biopeptide Co., San Diego, USA, and were of >95% purity, as evidenced by mass spectral analysis (MALDI-TOF Voyager).

2.2. Microorganisms

Escherichia coli ATCC 25922 was obtained from the Department of Clinical Bacteriology at Lund University Hospital, Sweden.

2.3. Viable-count analysis

E. coli ATCC 25922 was grown to mid-logarithmic phase in Todd-Hewitt (TH) medium. Bacteria were washed and diluted in 10 mM Tris, pH 7.4, 5 mM glucose, 0.15 M NaCl. 50 µl of 2×10^6 cfu/ml bacteria was incubated at 37 °C for 2 h in the presence of peptide at the indicated concentrations. Serial dilutions of the incubation mixture were plated on TH agar, followed by incubation at 37 °C overnight and cfu determination.

2.4. LPS effects on macrophages in vitro

Cells used were RAW 276.4 (ATCC TIB 71, American Type Culture Collection, Manassas, USA). 3.5×10^5 cells were seeded in 96-well tissue culture plates (Nunc, 167008) in phenol red-free DMEM

Table 1
Primary structure and key properties of the peptides investigated.

Holoprotein	Sequence	IP	Z _{net}	µH _{rel} (pH 7.4)	Z _{net} µH _{rel}
Coagulation factor IX (FIX)	KYGIYTKVSRVYV W IKEKTK	10.00	+5	0.41	2.05
Coagulation factor X (FX)	KYGIYTKVTAFLK W IDRSMK	10.00	+4	0.46	1.84
Coagulation factor XI (FXI)	RPGVYTNVVEYV D WILEKTQ	4.68	-1	0.40	-0.40
Kallikrein 5 (KLK5)	RPGVYTNLCKFT K WIQETIQ	9.20	+2	0.46	0.92
Kallikrein 8 (KLK8)	KPGVYTNICRYLD W IKKIIG	9.52	+3	0.45	1.35
Kallikrein 9 (KLK9)	RPAVYTSVCHYLD W IQEIME	4.65	-2	0.45	-0.90
Putative testis serine protease 5 (TSSP5)	NPGVYTRITKYTK W IKKQMS	10.30	+5	0.38	1.90
Hyaluronan-binding 2 (HABP2)	RPGVYTVTKFLN W IKATIK	10.46	+4	0.45	1.80
Coagulation factor II (Prothrombin) (THRB)	KYGFYTHVFR L KK W IQKVID	10.00	+4	0.46	1.84

IP: isoelectric point; Z_{net}: net charge; µH_{rel}: relative hydrophobic moment on the Kyte-Doolittle scale [35]. Conserved amino acids marked in bold.

(Gibco) supplemented with 10% FBS and antibiotics. Following 6 h of incubation to permit adherence, cells were stimulated with 100 or 10 ng/ml *E. coli* (0111:B4) (Sigma, St. Louis, USA), with and without peptide of various doses. The levels of NO in culture supernatants were determined after 24 h from stimulation using the Griess reaction [19]. Briefly, nitrite, a stable product of NO degradation, was measured by mixing 50 µl of culture supernatants with the same volume of Griess reagent (Sigma, G4410) and reading absorbance at 550 nm after 15 min. Phenol-red free DMEM with FBS and antibiotics were used as a blank. A standard curve was prepared using 0–80 µM sodium nitrite solutions in ddH₂O.

2.5. Liposome preparation and leakage assay

The liposomes investigated were anionic (DOPE/DOPG 75/25 mol/mol). DOPG (1,2-dioleoyl-*sn*-Glycero-3-phosphoglycerol, monosodium salt) and DOPE (1,2-dioleoyl-*sn*-Glycero-3-phosphoethanolamine) were from Avanti Polar Lipids (Alabaster, USA) and of >99% purity. The lipid mixture was dissolved in chloroform, after which solvent was removed by evaporation under vacuum overnight. Subsequently, 10 mM Tris buffer, pH 7.4, was added together with 0.1 M carboxy-fluorescein (CF) (Sigma, St. Louis, USA). After hydration, the lipid mixture was subjected to eight freeze-thaw cycles, consisting of freezing in liquid nitrogen and heating to 60 °C. Unilamellar liposomes of about 140 nm were generated by multiple extrusions (30 passages) through polycarbonate filters (pore size 100 nm) mounted in a LipoFast minixtruder (Avestin, Ottawa, Canada) at 22 °C. Untrapped CF was removed by two subsequent gel filtrations (Sephadex G-50, GE Healthcare, Uppsala, Sweden) at 22 °C, with Tris buffer as eluent. CF release from the liposomes was determined by monitoring the emitted fluorescence at 520 nm from a liposome dispersion (10 µM lipid in 10 mM Tris, pH 7.4). For the leakage experiment in the presence of LPS, 0.02 mg/ml LPS was first added to the above liposome dispersion (which did not cause liposome leakage in itself; results not shown), after which peptide was added and leakage monitored as a function of time. An absolute leakage scale was obtained by disrupting the liposomes at the end of each experiment through addition of 0.8 mM Triton X-100 (Sigma-Aldrich, St. Louis, USA). A SPEX-fluorolog 1650 0.22-m double spectrometer (SPEX Industries, Edison, USA) was used for the liposome leakage assay. Measurements were performed in triplicate at 37 °C.

2.6. CD spectroscopy

Circular dichroism (CD) spectra were measured by a Jasco J-810 Spectropolarimeter (Jasco, Easton, USA). The measurements were performed in duplicate at 37 °C in a 10 mm quartz cuvette under stirring with a peptide concentration of 10 μM. The effect on peptide secondary structure of liposomes at a lipid concentration of 100 μM was monitored in the range 200–260 nm. For measurements in the presence of LPS, 0.2 mg/ml was used. To account for instrumental differences between measurements, background subtraction was performed routinely. Signals from the bulk solution were also corrected for. Measurements were performed at 37 °C.

2.7. Ellipsometry

Peptide adsorption to supported lipid bilayers was studied in situ by null ellipsometry, using an Optrel Multiskop (Optrel, Kleinmachnow, Germany) equipped with a 100 mW argon laser. All measurements were carried out at 514 nm and an angle of incidence of 67.66° in a 5 ml cuvette under stirring (300 rpm). Both the principles of null ellipsometry and the procedures used have been described extensively before [20]. In brief, by monitoring the change in the state of polarization of light reflected at a surface in the absence and presence of an adsorbed layer, the mean refractive index (n) and layer thickness (d) of the adsorbed layer can be obtained. From the thickness and refractive index of the adsorbed amount (Γ) was calculated according to:

$$\Gamma = \frac{(n - n_0)d}{dn/dc} \quad (1)$$

where dn/dc is the refractive index increment and n_0 is the refractive index of the bulk solution. Corrections were routinely done for changes in bulk refractive index caused by changes in temperature and excess electrolyte concentration.

LPS-coated surfaces were obtained by adsorbing *E. coli* LPS to methylated silica surfaces (surface potential -40 mV, contact angle 90° [21]) from 5 mg/ml LPS stock solution in water at a concentration of 0.4 mg/ml over a period of 2 h. This results in a hydrophobically driven LPS adsorption of 0.8 mg/m², corresponding to plateau in the LPS adsorption isotherm under these conditions. Non-adsorbed LPS was removed by rinsing with Tris buffer at 5 ml/min for a period of 30 min, allowing buffer stabilization for 20 min. Peptide addition was performed at different concentrations of 0.01, 0.1, 0.5 and 1 μM, and the adsorption monitored for at least 1 h after each addition. All measurements were performed in at least duplicate at 25 °C.

Supported lipid bilayers were generated from liposome adsorption. DOPE/DOPG (75/25 mol/mol) were prepared as described above, but the dried lipid films resuspended in Tris buffer only with no CF present. In order to avoid adsorption of peptide directly at the silica substrate (surface potential -40 mV, and contact angle $<10^\circ$ [21]) through any defects of the supported lipid layer, poly-L-lysine ($M_w = 170$ kDa, Sigma-Aldrich, St. Louis, USA) was preadsorbed from water prior to lipid addition to an amount of 0.045 ± 0.01 mg/m², followed by removal of nonadsorbed poly-L-lysine by rinsing with water at 5 ml/min for 20 min [22]. Water in the cuvette was then replaced by buffer containing also 150 mM NaCl, which was followed by addition of liposomes in buffer at a lipid concentration of 20 μM, and subsequently by rinsing with buffer (5 ml/min for 15 min) when the liposome adsorption had stabilized. The final layer formed had structural characteristics (thickness 4 ± 1 nm, mean refractive index 1.47 ± 0.03), suggesting that a layer fairly close to a complete bilayer is formed. After lipid bilayer formation, temperature was raised and the cuvette content replaced by 10 mM Tris buffer at a rate of 5 ml/min over a period of 30 min. After stabilization for 40 min, peptide was added to a concentration of 0.01 μM, followed by three subsequent peptide additions to 0.1 μM, 0.5 μM, and 1 μM, in all cases monitoring the

adsorption for 1 h. All measurements were made in at least duplicate at 25 °C.

2.8. Dual polarization interferometry

Peptide adsorption to DOPE/DOPG supported bilayers were also investigated by dual polarization interferometry (DPI), using a Farfield AnaLight 4D (Biolin Farfield, Manchester, U.K.), operating with an alternating 632.8 nm laser beam. The technique is based on a dual slab waveguide, consisting of an upper sensing waveguide (supporting the lipid bilayer) and a lower reference waveguide. The changes induced by the peptide/lipid adsorption were monitored through changes in the transverse electric and transverse magnetic modes as described previously [23]. As for ellipsometry, Eq. (1) was used for determining the mass adsorbed, using refractive index increments of 0.135 and 0.182 cm³/g for lipid and peptide, respectively. Although treating phospholipids as optically isotropic systems is a reasonably accurate approximation for disorganized phospholipid bilayers, these actually display some optical birefringence, which is measurable with the sensitive DPI technique. The birefringence (Δn_f), obtained from the refractive indices for the TM and TE waveguide modes (assuming the bilayer thickness to be constant), reflects ordering of the lipid molecules in the bilayer, and decreases with increasing disordering of the bilayer [24,25]. Consequently, Δn_f can be used to monitor disordering transitions in lipid bilayers, e.g., as a result of peptide binding and incorporation, and therefore offers a simpler alternative to, e.g., order parameter analyses in ²H NMR spectroscopy [26]. In the present study, DOPE/DOPG liposomes (75/25 mol/mol) were prepared as described above for ellipsometry, and the liposomes (at a lipid concentration of 0.2 mg/ml in 10 mM HEPES buffer, containing also 150 mM NaCl and 1.5 mM CaCl₂) fused to the silicon oxynitride/silicon substrate (contact angle $<5^\circ$) at a flow rate of 25 μl/min for 8 min. This resulted in bilayer formation, characterized by a refractive index of 1.47, a thickness of 4.5 ± 0.3 nm, and an adsorbed amount of 4.4 ± 0.3 ng/mm² (the latter corresponding to an area per molecule of 54 Å²) (results not shown). After bilayer formation, current buffer was changed with 10 mM Tris buffer, allowing continuous flushing (at flow rate, 50 μl/min) for 10 min, after which peptide was added at the desired concentration. Peptide adsorption was monitored for 1 h. Measurements were performed at least in duplicate at 25 °C.

3. Results and discussion

In a previous study, we identified 68 S1 peptide sequences of potential interest as antimicrobial and host defense peptides [18]. From antimicrobial screening experiments, a number of these were found to display antimicrobial activities in low as well as physiological salt conditions. Broad spectrum activities of a number of the peptides were also demonstrated by results for Gram-negative *P. aeruginosa* and *E. coli*, Gram-positive *S. aureus*, and the fungus *C. albicans*. A number of the peptides were also found to possess anti-inflammatory properties, demonstrated by inhibition of NO release from macrophages stimulated by LPS or zymosan. In line with a range of AMPs, the antimicrobial activity of the S1-derived peptides was found to increase with the relative hydrophobicity (μH_{rel}) and the positive net charge (z_{net}). A similar correlation was found for the anti-endotoxic activity. Quantitative structure–activity relationship (QSAR) analysis showed that a number of descriptors significantly contributed to the antimicrobial and anti-endotoxic effect of these peptides, including net charge and hydrophobicity, as well as additional complex descriptors comprising electrostatic and hydrophobic components. The detailed mechanisms behind these effects remained unclear, however, e.g., regarding bacteria membrane rupture, binding competition of these peptides to LPS and phospholipid components in the bacteria membranes, and the correlation between LPS binding and anti-endotoxic effects of these peptides.

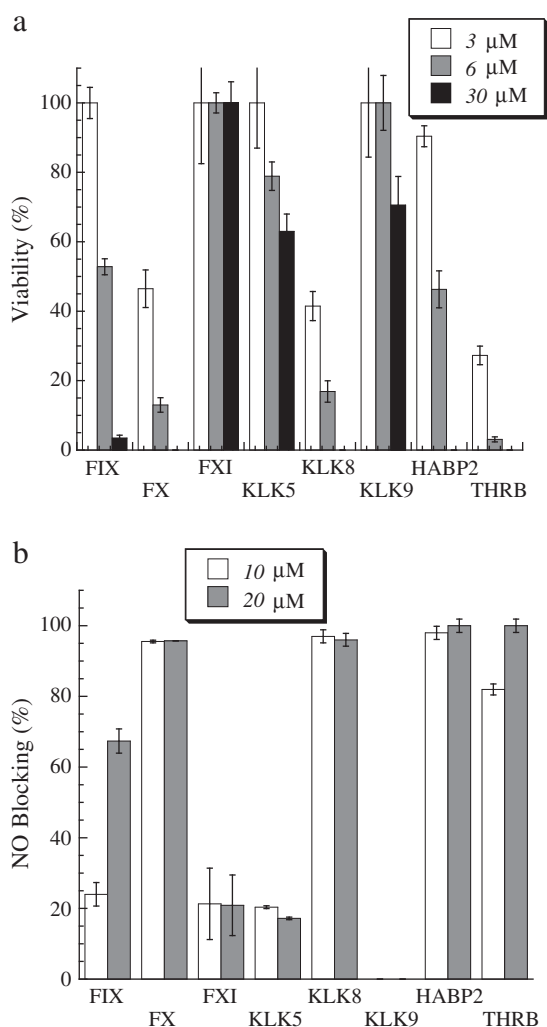


Fig. 1. (a) Antimicrobial effect, as determined by viable count assay in 150 mM NaCl, 10 mM Tris, pH 7.4, against Gram-negative *E. coli*. (b) Effects of the indicated peptides on NO production by macrophages. RAW264.7 mouse macrophages were incubated with LPS from *E. coli* in presence of peptides at the indicated concentration. NO production in the culture media 24 h after the treatment was determined using the Griess reagent.

In order to address these issues, we selected a series of S1-derived peptides, all of which display both antimicrobial and anti-endotoxic properties (Table 1 and Fig. 1), and all of which characterized by a high μH_{rel} and a net positive charge (z_{net}). As negative controls, we included also two peptides (from KLK9 and FXI, respectively), with high relative hydrophobic moment, but a net negative charge. As can be seen in Figs. 2 and S2, peptides derived from FIX, FX, KLK5, KLK8, THR8, TSSP5, and HABP2 all display concentration-dependent permeabilization of DOPE/DOPG liposomes, the TSSP5 peptide somewhat less so, while the net negatively charged FXI and KLK9 peptides do not lyse liposomes to any larger extent. From the comparison between antimicrobial effect and liposome lysis, it is clear that membrane disruption plays an important role in the antimicrobial activity of the investigated peptides (Fig. 1a), in line with findings of peptide-induced release of intracellular material for both *S. aureus* and *P. aeruginosa* caused by THR8, HABP2, and KLK8 peptides, absent for the FXI peptide [18]. In analogy to the findings on liposome rupture, the peptides from FX, KLK5, KLK8, THR8, and HABP2 all displayed high adsorption densities at DOPE/DOPG supported bilayers, while the TSSP5 peptide and even more so the

FXI peptide displayed somewhat lower adsorption densities, and the KLK9 peptide very low adsorption (Figs. 3 and S3). Quantitatively, and in line with previous findings [27], there is a correlation between the amount of peptide bound to the lipid membrane, and the extent of peptide-induced membrane disruption (Fig. 4a).

For all the peptides investigated, DPI experiments on DOPE/DOPG supported bilayers demonstrated a similar mode of membrane disruption. Thus, as shown in Figs. 5 and S4, peptide addition in all cases result in an essentially linear decrease in bilayer birefringence with an increasing peptide incorporation. In analogy to the ellipsometry experiments (although DPI giving slightly higher absolute values than ellipsometry), the saturation amounts differ between the different peptides, notably being much lower for the FXI and KLK9 peptides, but until that point is reached, a given amount of peptide incorporated induces the same degree of membrane disorganization. Importantly, there is no onset density, which means that peptides are incorporated into the membrane (as opposed to sitting on-top) throughout the binding process. This is analogous to results found for, e.g., aurein 1.2 on *E. coli* extract and DMPE/DMPG bilayers [25] and C3a C-terminal peptide CNYITELRRQLARASLLGLAR (CNY21L) on DOPC mono- and bilayers [28], and is expected from the relatively high hydrophobicity of the peptides investigated.

As shown in Figs. 3b and S3b, all peptides but that from KLK9, and to some extent also that from FXI, displayed extensive binding to *E. coli* LPS. Given the negative charge of the LPS carbohydrate region caused by phosphate and carboxylate groups [9], and the hydrophobicity introduced through its lipid A component, such extensive peptide binding may be caused by both electrostatic and hydrophobic interactions. Having said that, it should be noted that the LPS is likely to be anchored at the underlying hydrophobic surface through the lipid A component, in analogy to, e.g., structurally somewhat similar proteoglycans [29]. Since the LPS adsorption at the underlying hydrophobic surface is quite high (0.8 mg/m²), the lipid A moieties will therefore be at least partly screened by the LPS carbohydrate chains. Correlating the peptide adsorption to the LPS surface with the peptide net charge, mean hydrophobicity moment, and the product thereof, however, indicate that peptide binding to LPS is determined by both charge and hydrophobicity, the latter exemplified by LPS binding by the net negatively charged FXI peptide (Fig. 3b), while the latter is illustrated by the increasing LPS binding with increasing peptide net charge (Fig. 4b). Similarly, while adsorption of these peptides to the DOPE/DOPG membrane is determined also by peptide charge and hydrophobicity, ordered secondary structure induction at the membrane is correlated to high peptide binding (Fig. 4a), presumably due to the induced amphiphilicity of the induced helix (Figs. S5 and S6) providing an additional driving force for membrane incorporation. In parallel, the increased membrane binding displayed by the peptides able to form an amphiphilic helix, causes increased membrane lysis (Fig. 4a).

CD experiments demonstrate that the peptides investigated are largely disordered in buffer, with low (<15%; FIX, FX, THR8, TSSP5, KLK5, KLK9) or modest (15–20%; FXI, KLK8, HABP2) helix content. On binding to DOPE/DOPG liposomes, induction of ordered α -helix and β -sheet structures are found, notably for the FX, KLK5, KLK8, THR8, and HABP2 peptides (Figs. 6a and S5). Similarly, a number of the peptides result in pronounced helix signatures in the presence of LPS (Fig. 6b). Since many polysaccharides have the capacity of helix formation, and since LPS in itself displays a (albeit minor) CD signature, the helix formation observed could in principle be due either to the peptide, LPS, or the two components together. However, it has previously been demonstrated that peptides unable to form helices, but with otherwise structural features similar to those of the peptides investigated here, result in minor or no helix signatures in CD together with LPS [30]. The latter is supported also by findings of both truncations and of spaced D-amino acid substitutions in GK25 result in loss in helix induction of this peptide in the presence of

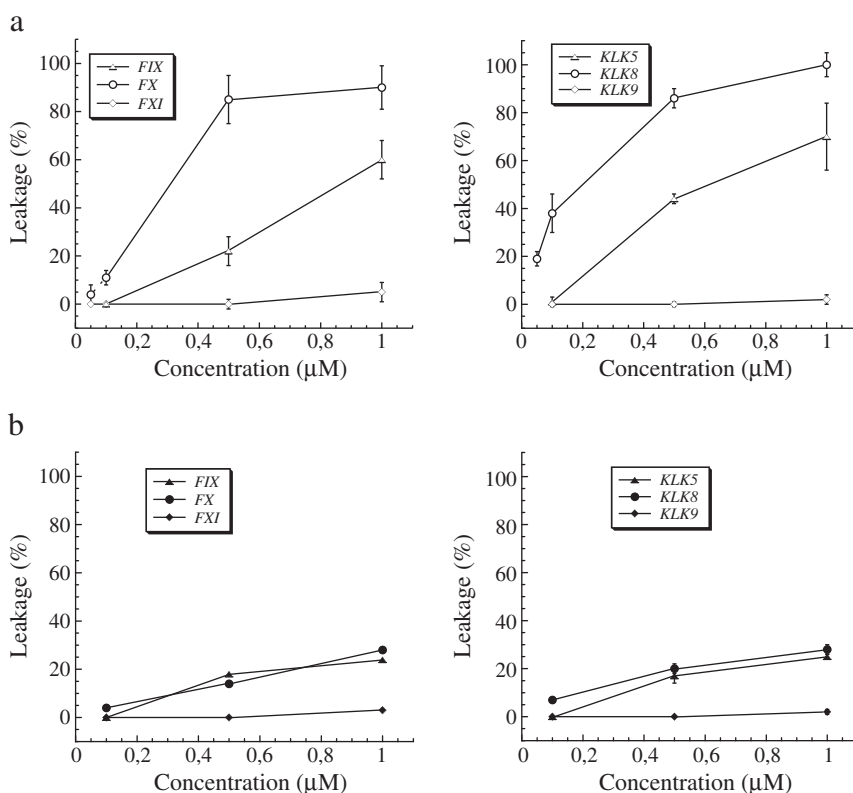


Fig. 2. Peptide-induced liposome leakage for DOPE/DOPG (75/25 mol/mol) in the absence (a) and presence (b) of 0.02 mg/ml *E. coli* LPS. Measurements were performed in 10 mM Tris, pH 7.4.

DOPE/DOPE and *E. coli* liposomes, as well as in the presence of LPS (to be published). Consequently, the helix induction here observed in the presence of LPS is primarily due to the peptide, and not LPS.

Given the extensive binding to both DOPE/DOPG bilayers and LPS of all but the FXI and KLK9 peptides, the next question is which of these are preferred for peptide binding. At first thought, the concentration increment of the peptide adsorption isotherms could provide this information, as could interpretation of the “on” and “off” rates on adsorption and desorption, respectively. However, due to strong electrostatic and hydrophobic interactions, dilution-induced peptide desorption from both DOPE/DOPG and LPS is quite limited, hence precluding analysis based on adsorption/desorption kinetics. Furthermore, due to the LPS molecules forming an adsorbed layer density distribution reaching into the bulk solution, while the DOPE/DOPG bilayer forming a largely 2-dimensional surface, the effective surface area of the two systems are not directly comparable. In addition, on binding of positively charged peptides to oppositely charged polyelectrolytes (such as LPS), there is generally a substantial contraction of the latter [31–33], thereby influencing the accessibility to further peptide binding. All these effects disqualify simple analysis based on the initial slope of the adsorption isotherm. Qualitatively, however, it is straightforward to elucidate which of LPS or the lipid membrane has the highest binding affinity for the peptides investigated. To demonstrate this, we compared peptide-induced liposome leakage in the absence and presence of LPS. In these experiments, LPS concentration was chosen as to not give any effect on liposome leakage in itself (results not shown). As can be seen in Figs. 2b and S2b, the presence of LPS caused a considerable reduction in peptide-induced liposome leakage for all peptides investigated, except for the net negatively charged FXI and KLK9 peptides. While this could, at

first sight, be taken to indicate increased resistance to peptide defect formation of LPS-containing membranes, this is unlikely, since LPS is added above its critical micellization concentration in these experiments, thus decreasing the driving force for LPS incorporation in the phospholipid membrane. Instead, the results indicate that the net positively charged peptides bind preferentially to LPS.

Comparing LPS binding to the anti-endotoxic effect of the peptides, it is worth noting that the negatively charged KLK9 peptide is unable to block LPS-induced NO production in macrophages (Fig. 1) [18]. All the other peptides, which bind to LPS, are able to block LPS-induced NO release to some extent. Of these, the weakly negatively charged FXI and the weakly positively charged KLK5 peptides display lower LPS binding than the higher charged peptides (e.g., FIX and HABP2), and also less blocking of LPS-induced NO release. Thus, LPS binding seems to be a necessary requirement for the anti-endotoxic effect of these peptides. An important question, however, is whether LPS binding is a sufficient requirement for the latter, i.e., whether the anti-endotoxic effect is merely an effect of “peptide scavenging”, e.g., through preventing “free” LPS to trigger the endotoxic cascade. While addressing this complex issue at any depth is outside the scope of the present investigation, and subject of ongoing studies to be reported separately, it is worth noting that NO blocking of the FIX peptide is significantly lower than that of e.g., the FX peptide (Fig. 1b). On the other hand, LPS binding of the FIX peptide is higher than that of the FX peptide (Fig. 3). While it should be noted that the direct comparison between the model biophysical experiments and those on cells should not be drawn too far due to methodologically motivated differences in, e.g., medium composition, the latter results indicate that LPS binding is a necessary condition for the anti-endotoxic effect of the presently investigated peptides, but not a sufficient one. The latter is indicated also by NO blocking by the FIX

and FX peptides being only marginally affected by the order of LPS and peptide addition (Fig. S7), despite this being expected to affect complex formation between LPS and peptide.

Although LPS covers >70% of the outer leaflet of Gram-negative bacteria [8], thereby constituting an important barrier for antimicrobial peptides before they can disrupt the inner plasma membrane and kill the bacteria, the interaction between antimicrobial peptides and LPS has only been relatively sparsely investigated in literature, at least beyond demonstrating LPS binding of various positively charged peptides [10,34]. There are, however, some good previous studies worth noting in this context. For example, Andr a et al. investigated the interaction of the antimicrobial peptide NK-2 and LPS, and found hydrophobic interactions to be necessary for efficient neutralization of the biological activity of LPS, but that the carbohydrate chains of LPS also provide electrostatically driven binding [14]. Similarly, the same authors found that C12 derivatization of the lactoferricin-derived peptide LF11 results in much stronger inhibition of LPS-induced cytokine generation [15]. The importance of both hydrophobic and electrostatic effects on the binding of LF11 to LPS was also found by Japelj et al. [16]. In a broad early investigation, Rosenfeldt et al. investigated the binding and anti-endotoxic effects of LL-37, magainin, and a 15-mer all-L synthetic K/L peptide and its D,L-counterpart [11]. These peptides were found to bind to LPS, and were suggested to disintegrate LPS aggregates (with the exception of magainin). It was suggested that anti-endotoxic effects of these peptides were accomplished through LPS binding and disintegration of LPS aggregates, thereby preventing (by unspecified mechanisms) LPS from binding the LPS-binding proteins of macrophages, and to trigger NF- κ B transcription factor activation. Interestingly, however, LPS binding in itself was not found to be sufficient for anti-endotoxic effect of these peptides. Furthermore, no correlation was observed

between the antimicrobial and anti-endotoxic properties of these peptides, suggesting that different peptide properties are needed for these activities. In a follow-up study, Rosenfeld et al. investigated a more homogenous set of K₆L₉ peptides with regard to charge distribution and D-substitutions [13]. While the effect of the size of the K and L “blocks” on LPS binding and disintegration was relatively minor, as were effects of partial D-substitutions in these peptides, the latter caused significant reduction in TNF- α generation. Since the helical and the disordered peptide variants displayed comparable LPS binding, the anti-endotoxic effect of these peptides seems to be related to the helix induction in the peptides for unknown reasons. For K₅L₇ peptides, on the other hand, the same authors reported the partly D-substituted peptide variant to display significantly lower LPS binding than the all-L variant [17], pointing to the importance of further studies of these effects. In a recent follow-up study, these authors continued their investigations with KL peptides (all containing 12 amino acids in total), this time varying the K/L ratio, and modifying the peptides with hexanoic and octanoic chains in order to further investigate the effects of peptide hydrophobicity [12]. With increasing acyl length, both antimicrobial and anti-endotoxin activity of the lipopeptide increased. Varying the K/L ratio resulted in less conclusive results, suggesting both peptide charge and hydrophobicity to be of importance to both antimicrobial and anti-endotoxic effect, thus increasing peptide hydrophobicity by replacing K with L at constant peptide length promotes hydrophobic interactions but simultaneously reduces electrostatic interactions.

Taken together, the results of the present study are largely in line with these previous findings. Thus, for the net negatively charged FXI and KLK9 peptides, the net electrostatic peptide-LPS repulsion dominates, reducing or eliminating LPS binding and NO production in macrophages. Similarly, the FXI and KLK9 peptides bound little or

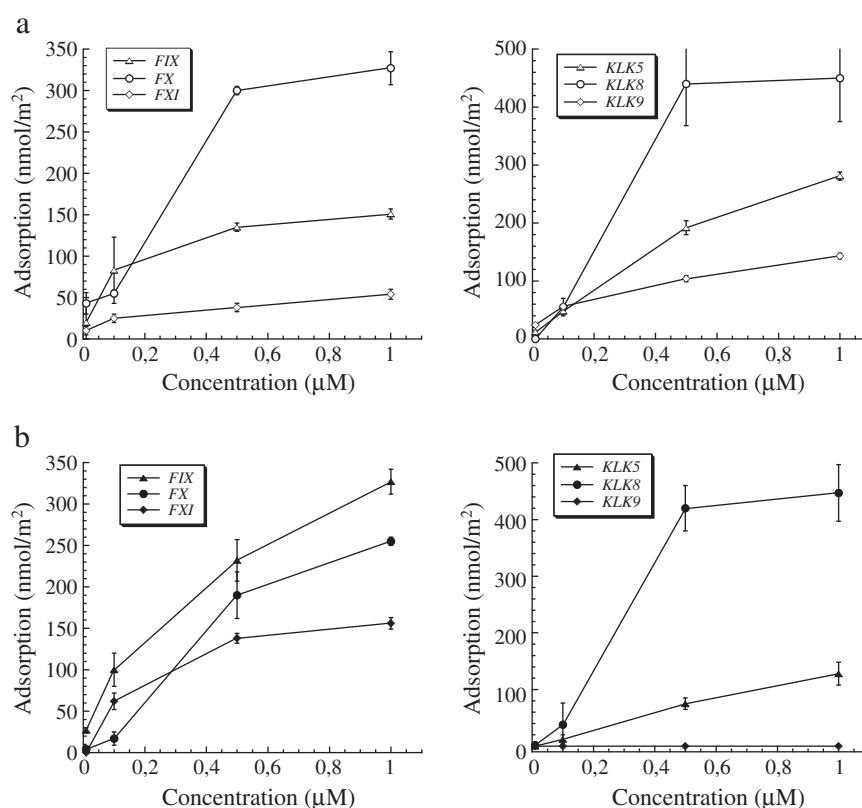


Fig. 3. Peptide binding to (a) supported DOPE/DOPG (75/25 mol/mol) bilayers, and (b) preadsorbed *E. coli* LPS ($\Gamma_{\text{LPS}} \approx 0.8 \text{ mg/m}^2$). Measurements were performed in 10 mM Tris, pH 7.4.

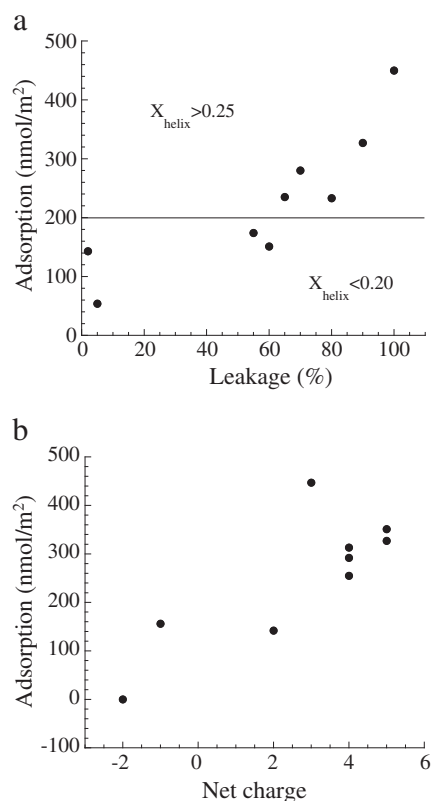


Fig. 4. (a) Correlation between DOPE/DOPG (75/25 mol/mol) liposome leakage induction and peptide adsorption density (both at a peptide concentration of 1 μ M) at the corresponding supported bilayers in 10 mM Tris, pH 7.4. Also indicated is the fractional helix content of the peptides in the presence of DOPE/DOPG liposomes (X_{helix}). (b) Correlation between peptide net charge and adsorption density at preadsorbed *E. coli* LPS ($\Gamma_{LPS} \approx 0.8$ mg/m²).

not at all to DOPE/DOPG bilayers, nor did they cause liposome lysis or potent bacterial killing. All the other peptides are characterized by a net positive charge and intermediate hydrophobicity, hence bind extensively to LPS (and DOPE/DOPG bilayers), and block NO production in macrophages. Similarly, the weakly positively charged KLK5 ($z_{net} = +2$) binds to LPS only sparingly, and block NO production modestly. Strikingly, however, while LPS binding increases somewhat with peptide net charge, this dependence is not

very strong, hence KLK8 ($z_{net} = +3$) displays higher LPS binding than both TSSP5 and FIX ($z_{net} = +5$), most likely an effect of the higher hydrophobic moment of KLK8, thus demonstrating an interplay between hydrophobic and electrostatic interactions. Analogously, NO blocking of KLK8 is the highest of the peptides investigated. Furthermore, as demonstrated by the LPS binding of FXI and the lack of such binding for KLK9, LPS binding seems to be a necessary but not sufficient criteria for anti-endotoxic effect, again in line with the studies discussed above. A common feature of the S1 peptides investigated is the conserved as well as varying hydrophobic amino acids, which are spaced so that helix formation is facilitated. The extent of helix induction in the presence of DOPE/DOPG varies between the peptides investigated, being high for KLK5, KLK8, THRB, FX, and HAMP2, but marginal for FIX and TSSP5, and correlates to liposome leakage induction and bacterial killing. Similarly, a dramatic helix induction is observed for all the peptides binding to LPS and causing NO blocking, suggesting a potential functional role of such secondary structure formation, in line with the previous findings discussed above.

4. Conclusions

For a series of structurally related peptides derived from the C-terminal region of S1 peptidases, antimicrobial and anti-endotoxic effects were investigated, and correlated to membrane defect formation in liposomes, to peptide binding to lipid membranes and LPS, and to secondary structure formation. Peptide-induced membrane lysis correlated to bacteria killing, and also to the amount of peptide incorporated into the lipid bilayer. Peptide binding to LPS and to lipid membranes (of which LPS was demonstrated to have the higher peptide binding affinity), in turn, depended on peptide net charge and hydrophobicity. Thus, net negatively charged peptides displayed low to very low binding to the negatively charged lipid membrane and to LPS, were unable to kill bacteria through lysis, and to block LPS-induced endotoxic effect. The dependence on the peptide net charge, however, is relatively weak, and a lower net positive charge can be balanced by higher peptide hydrophobicity. LPS binding was found to be necessary, but not sufficient, for anti-endotoxic effect of these peptides. Helix formation was observed in peptide/LPS complexes for all peptides displaying anti-endotoxic effect, and needs to be further investigated from a functional perspective. Similarly, helix formation was correlated to membrane binding, lysis, and antimicrobial effect of these peptides.

Supplementary data to this article can be found online at doi:10.1016/j.bbmem.2012.03.017.

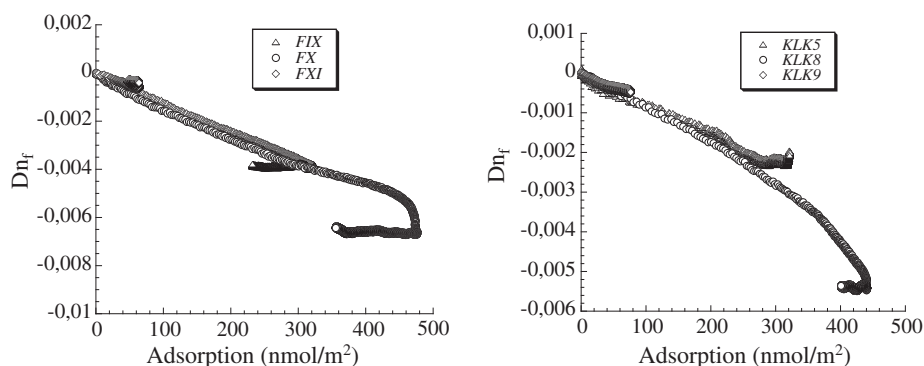


Fig. 5. Peptide-induced membrane disordering, monitored by DPI for DOPE/DOPG supported bilayers (75/25 mol/mol). Measurements were performed in 10 mM Tris, pH 7.4, and data reported as reduction in Δn_f , the lipid membrane birefringence, (due to peptide insertion) as a function of the adsorption density of the peptide.

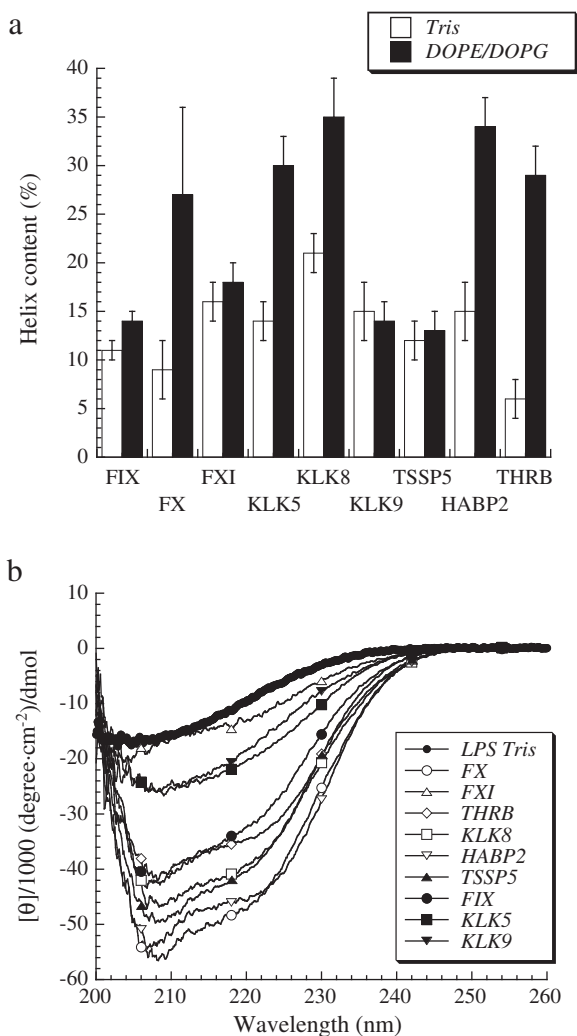


Fig. 6. (a) Helix content for the indicated peptides in buffer and in the presence of DOPE/DOPG liposomes. (b) CD spectra for the indicated peptides in the presence of *E. coli* LPS (0.2 mg/ml). Also CD spectrum for *E. coli* LPS 10 mM Tris, pH 7.4, is shown.

Acknowledgement

This work was supported by the Swedish Research Council (projects 621-2009-3009 and 521-2009-3378, 7480) and XImmune AB. Generous access to the DPI instrumentation from Biolin Farfield is gratefully acknowledged, as is valuable scientific discussion on the DPI results with Marcus Swann and Usha Devi at Biolin Farfield. Lise-Britt Wahlberg and Ann-Charlotte Strömdahl are gratefully acknowledged for technical support.

References

- [1] M. Zasloff, Antimicrobial peptides of multicellular organisms, *Nature* 415 (2002) 389–395.
- [2] R.E. Hancock, H.G. Sahl, Antimicrobial and host-defense peptides as new anti-infective therapeutic strategies, *Nat. Biotechnol.* 24 (2006) 1551–1557.
- [3] P. Elsbach, What is the real role of antimicrobial polypeptides that can mediate several other inflammatory responses? *J. Clin. Invest.* 111 (2003) 1643–1645.
- [4] M. Zanetti, Cathelicidins, multifunctional peptides of the innate immunity, *J. Leukoc. Biol.* 75 (2004) 39–48.
- [5] T. Ganz, Defensins: antimicrobial peptides of innate immunity, *Nat. Rev. Immunol.* 3 (2003) 710–720.
- [6] P. Papareddy, V. Rydengård, M. Pasupuleti, B. Walse, M. Mörgelin, A. Chalupka, M. Malmsten, A. Schmidtchen, Proteolysis of human thrombin generates novel host defense peptides, *PLoS Pathog.* 6 (e1000857) (2011) 1–15.
- [7] G. Kasetty, P. Papareddy, M. Kalle, V. Rydengård, M. Mörgelin, B. Albiger, M. Malmsten, A. Schmidtchen, Structure-activity studies and therapeutic potential of

- host defense peptides of human thrombin, *Antimicrob. Agents Chemother.* 55 (2011) 2880–2890.
- [8] D.S. Snyder, T.J. McIntosh, The lipopolysaccharide barrier: correlation of antibiotic susceptibility with antibiotic permeability and fluorescent probe binding kinetics, *Biochemistry* 39 (2000) 11777–11787.
- [9] E. Schneck, E. Papp-Szabo, B.E. Quinn, O.V. Kononov, T.J. Beveridge, D.A. Pink, M. Tanaka, Calcium ions induce collapse of charged O-side chains of lipopolysaccharides from *Pseudomonas aeruginosa*, *J. R. Soc. Interface* 6 (2009) S671–S678.
- [10] Y. Rosenfeld, Y. Shai, Lipopolysaccharide (endotoxin)-host defense antibacterial peptides interactions: role in bacterial resistance and prevention of sepsis, *Biochim. Biophys. Acta* 1758 (2006) 1513–1522.
- [11] Y. Rosenfeld, N. Papo, Y. Shai, Endotoxin (lipopolysaccharide) neutralization by innate immunity host-defense peptides, *J. Biol. Chem.* 281 (2006) 1636–1643.
- [12] Y. Rosenfeld, N. Lev, Y. Shai, Effect of the hydrophobicity to net positive charge ratio on antibacterial and anti-endotoxin activities of structurally similar antimicrobial peptides, *Biochemistry* 49 (2010) 853–861.
- [13] Y. Rosenfeld, H.-G. Sahl, Y. Shai, Parameters involved in antimicrobial and endotoxin detoxification activities of antimicrobial peptides, *Biochemistry* 47 (2008) 6468–6478.
- [14] J. Andrä, M.H. Koch, R. Bartels, K. Brandenburg, Biophysical characterization of endotoxin inactivation by NK-2, an antimicrobial peptide derived from mammalian NK-lysin, *Antimicrob. Agents Chemother.* 48 (2004) 1593–1599.
- [15] J. Andrä, K. Lohner, S.E. Blondelle, R. Jerala, I. Moriyon, M.H. Koch, P. Garidel, K. Brandenburg, Enhancement of endotoxin neutralization by coupling of a C12-alkyl chain to a lactoferrin-derived peptide, *Biochem. J.* 385 (2005) 135–143.
- [16] B. Japelj, P. Pristovsek, A. Majerle, R. Jerala, Structural origin of endotoxin neutralization and antimicrobial activity of a lactoferrin-based peptide, *J. Biol. Chem.* 280 (2005) 16955–16961.
- [17] N. Papo, Y. Shai, A molecular mechanism for lipopolysaccharide protection of Gram-negative bacteria from antimicrobial peptides, *J. Biol. Chem.* 280 (2005) 10378–10387.
- [18] G. Kasetty, P. Papareddy, M. Kalle, V. Rydengård, B. Walse, B. Svensson, M. Mörgelin, M. Malmsten, A. Schmidtchen, The C-terminal sequence of several human serine proteases encodes host defense function, *J. Innate Immun.* 3 (2011) 471–482.
- [19] J.S. Pollock, U. Forstermann, J.A. Mitchell, T.D. Warner, H.H. Schmidt, M. Nakane, F. Murad, Purification and characterization of particulate endothelium-derived relaxing factor synthase from cultured and native bovine aortic endothelial cells, *Proc. Natl. Acad. Sci. U. S. A.* 88 (1991) 10480–10484.
- [20] M. Malmsten, Ellipsometry studies of protein layers adsorbed at hydrophobic surfaces, *J. Colloid Interface Sci.* 166 (1994) 333–342.
- [21] M. Malmsten, N. Burns, A. Veide, Electrostatic and hydrophobic effects of oligopeptide insertions on protein adsorption, *J. Colloid Interface Sci.* 204 (1998) 104–111.
- [22] L. Ringstad, A. Schmidtchen, M. Malmsten, (2006) Effect of peptide length on the interaction between consensus peptides and DOPC/DOPA bilayers, *Langmuir* 22 (2006) 5042–5050.
- [23] A. Mashagi, M. Swann, J. Popplewell, M. Textor, E. Reimhult, Optical anisotropy of supported lipid structures probed by waveguide spectroscopy and its application to study of supported lipid bilayer formation kinetics, *Anal. Chem.* 80 (2008) 3666–3676.
- [24] L. Yu, L. Guo, J.L. Ding, B. Ho, S.-S. Feng, J. Popplewell, M. Swann, T. Wohland, Interaction of an artificial antimicrobial peptide with lipid membranes, *Biochim. Biophys. Acta* 1788 (2009) 333–344.
- [25] T.-H. Lee, C. Heng, M.J. Swann, J.D. Gehman, F. Separovic, M.-I. Aguilar, Real-time quantitative analysis of lipid disordering by aurein 1.2 during membrane adsorption and lysis, *Biochim. Biophys. Acta* 1798 (2010) 1977–1986.
- [26] G. Orädd, A. Schmidtchen, M. Malmsten, Effects of peptide hydrophobicity on its incorporation in phospholipid membranes – an NMR and ellipsometry study, *Biochim. Biophys. Acta* 2011 (1808) (2010) 244.
- [27] A.A. Strömstedt, L. Ringstad, A. Schmidtchen, M. Malmsten, Interaction between amphiphilic peptides and phospholipid membranes, *Curr. Opin. Colloid Interface Sci.* 15 (2010) 467–478.
- [28] L. Ringstad, E. Protopapa, B. Lindholm-Sethson, A. Schmidtchen, A. Nelson, M. Malmsten, An electrochemical study into the interaction between complement-derived peptides and DOPC mono- and bilayers, *Langmuir* 24 (2008) 208–216.
- [29] M. Malmsten, P. Claesson, G. Siegel, Forces between sulphate layers adsorbed at hydrophobic surfaces, *Langmuir* 10 (1994) 1274–1280.
- [30] P. Papareddy, M. Kalle, G. Kasetty, M. Mörgelin, V. Rydengård, B. Albiger, K. Lundqvist, M. Malmsten, A. Schmidtchen, C-terminal peptides of tissue factor pathway inhibitor are novel host defense molecules, *J. Biol. Chem.* 36 (2010) 28378–28398.
- [31] H. Bysell, P. Hansson, M. Malmsten, Effect of charge density on the interaction between cationic peptides and oppositely charged microgels, *J. Phys. Chem. B* 114 (2010) 7207–7215.
- [32] H. Bysell, P. Hansson, A. Schmidtchen, M. Malmsten, Effect of hydrophobicity on the interaction between antimicrobial peptides and poly(acrylic acid) microgels, *J. Phys. Chem. B* 114 (2010) 1307–1313.
- [33] H. Bysell, A. Schmidtchen, M. Malmsten, Binding and release of consensus peptides by poly(acrylic acid) microgels, *Biomacromolecules* 10 (2009) 2162–2168.
- [34] M. Pasupuleti, A. Schmidtchen, A. Chalupka, L. Ringstad, M. Malmsten, End-tagging of ultra-short antimicrobial peptides by W/F stretches to facilitate bacterial killing, *PLoS One* 4 (e5285) (2009) 1–9.
- [35] J. Kyte, R.F. Doolittle, A simple method for displaying the hydropathic character of a protein, *J. Mol. Biol.* 157 (1982) 105–132.